Targeting Shape and Material in Lighting Design

Usta, B.; Pont, S.; Eisemann, E.

DOI
10.1111/cgf.14678

Publication date
2022

Document Version
Final published version

Published in
Computer Graphics Forum

DOI: 10.1111/cgf.14678
Pacific Graphics 2022
N. Umetani, E. Vouga, and C. Wojtan
(Guest Editors)

Volume 41 (2022), Number 7

Targeting Shape and Material in Lighting Design

B.Usta[1] †, S. Pont[2], and E. Eisemann[1]

[1] Computer Graphics and Visualization Lab, Delft University of Technology, The Netherlands
[2] Perceptual Intelligence Lab, Delft University of Technology, The Netherlands

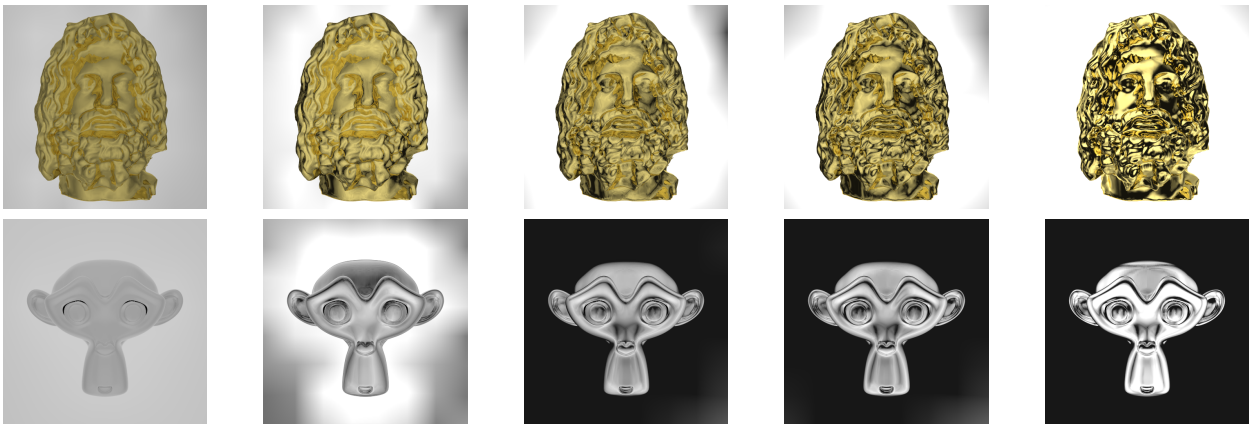

(a) *AG = 1* **(b)** *AG = 2* **(c)** *AG = 3* **(d)** *AG = 4* **(e)** *AG = 10*

Figure 1: *Two objects made of mirror materials under different environment maps generated by our system. F.l.t.r: illumination is optimized to produce a more reflective look using the user-specified Apparent Gloss (AG) parameter.*

Abstract

Product lighting design is a laborious and time-consuming task. With product illustrations being increasingly rendered, the lighting challenge transferred to the virtual realm. Our approach targets lighting design in the context of a scene with fixed objects, materials, and camera parameters, illuminated by environmental lighting. Our solution offers control over the depiction of material characteristics and shape details by optimizing the illuminating environment-map. To that end, we introduce a metric that assesses the shape and material cues in terms of the designed appearance. We formalize the process and support steering the outcome using additional design constraints. We illustrate our solution with several challenging examples.

CCS Concepts

• ***Computing methodologies*** → ***Computational photography; Image processing; Perception;***

1. Introduction

Traditional product photography uses complex lighting setups to achieve a desired result, often involving expensive equipment; a lengthy and laborious setup process [HBF12b]. For this reason, creating and rendering virtual counterparts has become a standard procedure in product design. Nevertheless, even in a virtual setting, controlling lighting effectively is a challenge.

Light designers commonly employ an environment map to simulate the complexity of natural environmental lighting. However, choosing or designing such a map to reveal the desired appearance is difficult. By directly editing the map, the resulting image can only be indirectly influenced. It requires expertise with corresponding tools for editing the environment map efficiently, as well as in-depth knowledge regarding the interaction of light and material to steer the process. Here, we present an automated system that assists artists in environment map design for scenes with fixed objects, materials, and camera parameters.

† {b.usta,s.pont,e.eisemann}@tudelft.nl

On the one hand, lighting designers, pursue artistic goals such as creating a mood or delivering a message by drawing attention to a specific region. Our solution therefore offers a painting metaphor to specify a target brightness for regions of interest, similar to [ADW04], which are respected during the derivation of the environment map.

By arranging the lighting carefully, the appearance of shape and material can be heavily influenced. Lighting designers can aim to emphasize or hide various object characteristics through lighting to, e.g., create attractive product photographs for e-commerce.

We propose a method to control apparent shape and material simultaneously based on the concept of shading flow [BZ96]. Instead of reconstructing shape from shading, we optimize the environment map to realise a desired appearance. We note that image gradients can represent shape and material cues, which we optimize in our framework by producing a suitable environment map based on a novel cost function. Further, we introduce *Apparent Gloss* (*AG*) parameter that can strongly impact the material impression. This parameter can be applied locally and leads to an environment map that makes even a glossy object appear diffuse (equal 1) or increasingly glossy (larger than 1) by optimizing the environmental illumination accordingly. Hereby, we can influence the local surface appearance albeit not changing the actual material properties.

Specifically, we make the following contributions:

- A system to define lighting design goals using a painting-based interface;
- An environment-map optimization framework to satisfy design goals;
- A cost function that covers material and shape cues.

2. Related Work

Here, we will discuss principles of lighting design, digital lighting design interfaces, and computer-aided solutions.

Lighting Design Principles Digital product lighting designers follow guidelines [HBF12b] relating to the underlying shape, material and goals for visually communicating the product properties.

Light interacts with scene geometry and material and produces several visual features such as smooth shading, specular highlights, and shadow boundaries. These features contribute to a viewers' scene understanding and shape perception but the exact role of each visual cue has not been well understood [CF07]. Different combinations of visual cues can result in the same perceived shape and material. People utilize various assumptions to infer shape among a range of solutions [KDKT01]. One important visual cue that leads to a stable shape perception among viewers [KHA*18] are high image gradients at critical contours, where the surface is strongly curved. Relative pixel intensities are also crucial for perceiving local surface structure [JP94]. Specular highlights [FTA04; WP10] and their orientation [KMA11] can provide cues regarding surface orientation. By manipulating such visual cues, one can depict a surface as flatter or more curved [MA14]. We aim to exploit these mechanisms for lighting design.

Fleming et al. argue that humans can infer even the shape of glossy materials, namely mirror objects, with great success [FTA04], based on the distortion of the reflections. Our approach combines shading gradients and distorted reflections to pronounce the shape of metal objects.

General cues for perceived glossiness for rendered images have been heavily studied; contrast and sharpness being the most effective ones [PFG00; WAKB09]. In fact, if they are not in line with the objects' diffuse shading, our perception of the material is diminished [KMA11; SN18]. In addition, if reflections exhibit real-world statistics, humans perform better in inferring the object glossiness [FDA03; vAWP16]. Image histogram skewness was proposed to quantify the perceived glossiness [MNSA07], but some reported contradicting findings [WP10; AK09].

Illumination patterns can influence glossiness perception [DBM07; WP10; ZdRBP19] and blurred environment maps can make glossy materials appear matte [DBM07]. However, such an operation is difficult to control or quantify. Bousseau et al. [BCRA11] developed metrics for producing a lighting setup emphasizing the glossy appearance. Their metric for metals and materials that exhibit strong Fresnel effects only maximizes total image gradients ignoring curvature and spatial image relations. Thus, it does not necessarily capture contrast, sharpness, or orientation of highlights. Notice a sharp gradient over a set of pixels and a gray image with noise can have the same total image gradient.

Figure 2: *Left and middle: Glass-object photograph with highlighted contours, small specular reflections are avoided and the background has a constant color (usually black or white). Right: An additional highlight on the body can serve to emphasise the shape [HBF12a].*

Glass is one of the most challenging materials to depict, as it is both reflective and refractive. It can produce confusing features leading to an ambiguous material perception for complex structures [TN19]. Professional photographers typically use a setup, where only contours are highlighted and the center is free from specular highlights [HBF12a] (Fig. 2 left, middle). In such a scenario, only the shape's silhouette is well visible and designers specifically aim for a simple dark or white background visible through the shape. Still, a specular highlight on a glass bottle could be preferred for certain product presentation goals (Fig. 2 right).

Digital Lighting Design Interfaces Kerr and Pellacini [KP09] suggest that there are three types of interfaces for digital lighting design; direct, indirect, and painting-based. In the first, artists directly manipulate light-source parameters. The second enables direct modification of visual features (shadows, highlights, ambient

color) [Pel10; BPB13] and an optimizer determines the light parameters. Finally, in painting-based solutions, desired visual features are drawn on the image and a lighting setup that produces the appearance is found through optimization [PRJ97; ADW04; PBMF07]. Kerr and Pellacini argue that despite its ease of use, painting-based interfaces are not superior because users are required to paint accurately to obtain satisfactory results, which is challenging for novice users. Our painting-based interface does not require such precision.

Computer-aided lighting design Many automatic solutions find optimal light parameters to satisfy user requirements for shape depiction [SL01; LHV06; WK13; WVBT16], material depiction [SL01], and aesthetics [PBMF07; LGCB14; GLCC18]. However, these solutions focus on a few light sources. Other approaches enable indirect modifications of the environment maps by selecting features in the image [Pel10]. Yet, a local change can have global impact. Instead, a suitable environment map can be produced based on various constraints from scratch [BCRA11]. We adopt such a solution and illustrate the effectiveness of integrating shape cues.

Compositing solutions [FA07; BPB13] offer a large degree of freedom but can fail to produce convincing and physically-correct images (e.g., different light sources for different image regions).

3. Optimization Framework

Our framework enables users to design environment maps using simple view annotations that allow local appearance design. Fig. 3 shows an overview of our framework. A typical design session starts with a few user annotations for the apparent shape and material design. Depending on how the optimizer progresses, the user interferes with the process and iterates the design or updates the global parameters. We refer to our supplementary video for an illustration of the interaction with the system. Here, we will first explain its principles and then introduce the design tools.

Our goal is to support three design goals; shape-material, pixel brightness and total luminosity, but our solution is extendable, similar to [SL01]. These targets are met by deriving an environment map w such that the resulting image $I(w)$ minimizes a cost function C. The cost function is a linear combination of separate cost functions C_i with user-defined weights β_i: $C = \beta_{SM}C_{SM} + \beta_B C_B + \beta_L C_L$, according to the above-defined three design goals. These weights come with default values but are made available in the interface to the user to give more fine-grained control over the optimization process.

To avoid rendering costs during optimization, we pre-integrate the light transport in the image domain following [BCRA11]. We produce a matrix T, in which each column corresponds to the resulting image pixels, when illuminated with a single texel of the environment map w. We can compute the final image $I(w)$ by multiplying the environment map w with T: $I(w) = Tw$.

3.1. Shape-Material Cost Function

Lighting affects how shape and material appear. However, they are interdependent since changing one can influence the other's appearance. A lighting designer has to consider both simultaneously.

Following [BZ96], the image gradient can be linked to shape and material appearance. Their assumption is that the shading gradient is only caused by the orientation difference between surface patches at each pixel, ignoring interreflections and shadows. We will build upon these insights to derive a cost function that gives control over the glossiness appearance of a model, which we introduce in the following.

3.1.1. Diffuse Appearance

Given a single light direction and considering only diffuse shading, a uniformly colored patch in an image is a likely indication of a flat region, while a gradient in a certain direction implies a curving of the surface along that direction. Our goal is to derive a cost function that favors gradients along the curving diffuse surface. For this, we will first describe the derivation of a goal gradient that captures the expected gradients of the object depicting its shape. We propose two methods, the first samples the result by rendering various images of the scene, the second is an analytical derivation. The goal gradients will then be used to define the cost function that penalizes deviations from the expected appearance.

Sample-Based Goal Gradients One way to estimate the expected appearance of a diffuse object is to render the scene using a diffuse white material under various directional light orientations and analyze the resulting image gradients. For each pixel, we hereby collect gradient samples. In order to capture the general orientation of the shading gradients we perform a PCA for each pixel considering the renderings that produce a nonzero gradient. The first component of the PCA gives the orientation of the larger gradients, which is the orientation of the view-dependent principal curvature, λ_p. View-dependent curvature measures the visible bending of a surface [JDA07]. Additionally, we calculate the expected gradient magnitude, $E[|\nabla I_p|]$, using the same nonzero gradient samples by averaging the absolute magnitude of projected gradient samples onto the first component of the PCA. Finally, we define the goal diffuse shading gradient for pixel p as $G_p = \lambda_p * E[|\nabla I_p|]$. Please note that the shading largely varies along the principle direction of the view-dependent curvature but the same curving surface can lead to a gradient from light to dark or dark to light, depending on the position of the light source. For this reason, only the expected magnitude is of relevance.

Normal-Based Goal Gradients To avoid sampling, we also present an analytical derivation of a goal gradient. Nevertheless, this technique disregards shadows and interreflections and purely considers surface orientation.

The pixel's value $I_p(\phi)$ on a diffuse surface with reflectance ρ receiving light from direction ϕ with intensity one is given by $I_p(\phi) = \rho max(0, n_p\phi)$, where n_p is the object's normal in pixel p. To simplify notations, we assume $\rho = 1$.

We now describe the derivation of normal-based $E[|\nabla I_p|]$, the expected gradient magnitude. We approximate it calculating for both the horizontal and vertical neighbor and taking the maximum since it is closer to the orientation of λ. Two horizontal neighboring pixels p, q whose normals n_p, n_q have an angular difference θ can either point towards each other (concave) or away from each

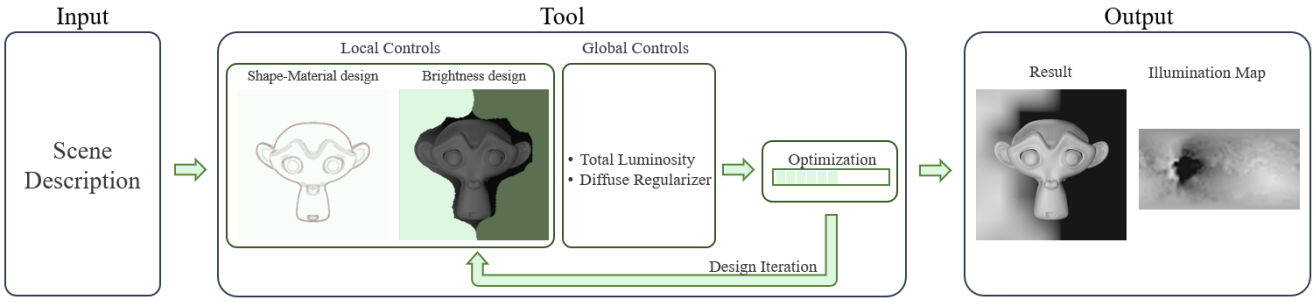

Figure 3: *Overview. Starting with a 3D scene description, the user can locally design Shape-Material appearance and brightness using painting interfaces. The user can further guide the optimizer by specifying global parameters. Then, our optimizer searches for an environment map that satisfy the design goals. During optimization, the user can step in and update their design until being satisfied.*

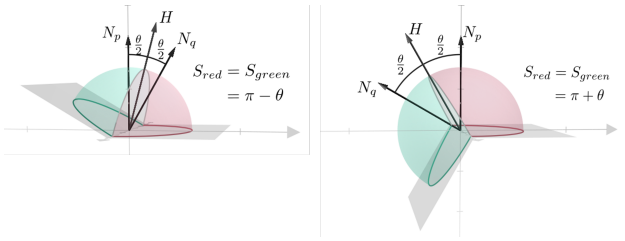

Figure 4: *Concave (left) and convex (right) cases are treated separately to compute $E[|\nabla I_p|]$.*

other (convex). We calculated convex and concave cases separately because in the latter case, neighbor patches occlude each other for some illumination directions. Due to symmetry, only half the light directions need to be considered to determine $E[|\nabla I_p|]$ (green in Fig. 4).

To proceed, in deriving $E[|\nabla I_p|]$, we assume two adjacent patches with their corresponding normals. For each light direction, we want to determine the shading difference, thus the resulting image gradient. Averaging these differences will allow us to conclude on the expected gradient magnitude.

To derive the result, we group the light directions according to whether a surface patch is lit or not, which determines the integration bounds. This enables us to eliminate the norm around the cosine evaluation (Fig. 4). First, we consider the concave case:

$$
\begin{aligned}
E[|\nabla I_p|] &= \frac{1}{\pi\text{-}\theta}\int_0^{\pi}\sin(\beta)\int_{-\frac{\theta}{2}}^{\frac{\pi}{2}\text{-}\theta}\sin(\beta)(\cos(\alpha)\text{-}\cos(\alpha+\theta))\,d\alpha d\beta \\
&= \frac{1}{\pi\text{-}\theta}\int_0^{\pi}\sin(\beta)^2\left(\sin(\alpha)\text{-}\sin(\alpha+\theta)\Big|_{-\frac{\theta}{2}}^{\frac{\pi}{2}\text{-}\theta}\right)d\beta \\
&= \frac{1}{\pi\text{-}\theta}\int_0^{\pi}\sin(\beta)^2(2\sin(\frac{\theta}{2})+\sin(\frac{\pi}{2}\text{-}\theta)\text{-}1)\,d\beta \\
&= \frac{\pi(2\sin(\frac{\theta}{2})+\sin(\frac{\pi}{2}\text{-}\theta)\text{-}1)}{2(\pi\text{-}\theta)}
\end{aligned}
$$

where α and β represent the azimuth and the altitude respectively. Second, the convex case, with adjusted bounds, yields:

$$
\begin{aligned}
E[|\nabla I_p|] &= \frac{1}{\pi+\theta}\int_0^{\pi}\sin(\beta)\int_{-\frac{\theta}{2}}^{\frac{\pi}{2}}\sin(\beta)(\cos(\alpha)\text{-}\cos(\alpha+\theta))\,d\alpha d\beta \\
&= \frac{1}{\pi\text{-}\theta}\int_0^{\pi}\sin(\beta)^2\left(\sin(\alpha)\text{-}\sin(\alpha+\theta)\Big|_{-\frac{\theta}{2}}^{\frac{\pi}{2}}\right)d\beta \\
&= \frac{1}{\pi+\theta}\int_0^{\pi}\sin(\beta)^2(2\sin(\frac{\theta}{2}))d\beta = \frac{\pi\sin(\frac{\theta}{2})}{(\pi+\theta)}
\end{aligned}
$$

Lastly, on the countour of the object, we have pixels without a visible neighbor patch. We assume the normal is $-n_p$ and compute $E[|\nabla I_p|]$ as 0.5 using the convex case formula with the angular difference π.

3.1.2. Glossy Appearance

We have seen that diffuse surfaces would lead to a gradient of $E[|\nabla I_p|]$, while the presence of highlights implies a larger contrast. By scaling the goal gradient magnitude with our parameter AG_p, we can implicitly control the depicted glossiness at pixel p. As we set the light source's intensity to one, a gradient cannot be larger than one. Thus, we allow scaling the goal gradient, such that $|\bar{G}_p| = 1$. This scaling can be locally applied by defining corresponding masks. Thus, the goal gradient is defined as $\bar{G}_p = min(\frac{1}{|G_p|}, AG_p) * \lambda_p * E[|\nabla I_p|]$. AG enables us to design various apparent gloss; $AG = 0$ produces flat appearance, $AG < 1$ less curved diffuse appearance, $AG = 1$ diffuse appearance for the designed shape appearance and $AG > 1$ results in glossy appearance (the higher is the glossier).

3.1.3. Cost Function

Our shape-material cost function consists of two terms evaluating different aspects of a given environment map; $C_{SM} = C_{SM_1} + \beta_{SM_2} C_{SM_2}$.

C_{SM_1} calculates the distance between image gradient and calculated goal gradient $\bar{G}$ while satisfying three objectives. First, the gradient should follow the goal orientation. Second, since we focus on shape appearance while supporting the designed material, a nonzero gradient is preferred over a zero gradient if it fol-

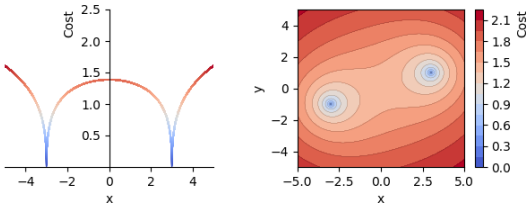

Figure 5: *Shape-material cost function behavior for a 1D goal (x:3) and a 2D goal (x:3, y:1) in left and right respectively*

lows the expected direction. Thirdly, image gradient should not be larger than a maximum value because of the light intensity one assumption. A way to achieve this is to penalize pixels with gradients larger than their goal gradients. The last criterion ensures that the cost of large gradient magnitudes do not dominate the total cost. The term $C_{SM_1} = \frac{1}{\sum_i log(1+|\bar{G}_i|)} \sum_i M_{SM} log(1 + \sqrt{|\bar{G}_i - \nabla I_i||\bar{G}_i - \nabla I_i|})$ satisfies all conditions, where M_{SM} is a binary mask that selects relevant pixels for the error calculation (See Fig. 5).

The second term C_{SM_2}, called diffuse regularizer, handles a special minima; alternating bright and dark pixels would satisfy the first term with $\measuredangle G_p = 1$ because we need to work with the magnitude to handle the orientation ambiguity. This solution does certainly not produce a diffuse appearance. Nevertheless, this solution requires a low frequency pattern in the environment map. Using a regularization in form of minimizing the spatial difference in the environment map ensures that the optimizer is guided correctly. For this term, we first calculate the spatial difference matrix H for an equilateral environment map as

$$H_{i,j} = \begin{cases} \sum arccos(d_i * d_j), & \text{if } i = j \\ -arccos(d_i * d_j), & \text{otherwise,} \end{cases}$$

where d_i is the vector to the i'th texel center. Secondly, we calculate spatial difference weight, b_i, for each environment-map texel by analyzing $\measuredangle G$ values designed for the image pixels that i'th texel illuminates. Taking the minimum, $\measuredangle G_{min_i}$, we define $b_i = \frac{1}{n} max(0, \gamma - min(\measuredangle G_{min_i}))$ where n is the number of environment-map texels and γ controls the $\measuredangle G$ range where the regularizer is effective. We set $\gamma = 2$ in our test cases.

3.2. Brightness Cost Function

Customized local lighting specifications are of high relevance to designers [ADW04]. Our solution supports defining a local target brightness (e.g., to highlight a label on a bottle or imposing a strong contrast between fore- and background). One option is to define the cost function for a pixel i as the absolute difference between I_i and the target brightness B_i. However, human brightness perception is not linear. Thus, we map the brightness values to a perceptually linear space and define the brightness cost function as:
$C_B = \frac{1}{|\{i|B_i \neq 0\}|} \sum \delta_i (I_i(w)^\gamma - B_i^\gamma)^2$, with $\gamma = 0.5$ following Steven's Power Law and δ_i is a per-pixel strength that allows to place local importance on the brightness goals.

While other systems [KP09] require a very careful and precise annotation for high quality results, our solution is more forgiving towards annotation mistakes due to the effective shape-material design.

3.3. Total Luminosity Cost Function

Our last cost function term C_L controls the total luminosity of the environment map via the user-specified parameter L. Hereby, the overall appearance can be influenced, such as a metal look under bright illumination or a diffuse look under dark illumination. Additionally, it helps keeping the result within the displayable range. Since the environment pixels are only indirectly influencing the final image, we adopted an L2 cost function. It is calculated as $C_L = \frac{1}{n}(L - \sum^n a_j * w_j)^2$ where a_j is the solid angle and w_j is the value of the environment map's j'th texel.

4. Implementation

We implemented our solution in C++ using OpenCV [Bra00] on an Intel i7-8700 CPU with 16GB of RAM, NVIDIA GTX 1080TI GPU, and Windows 10.

We initialize the Light Transport Matrix T and normals per pixel using PBRT [PH10]. For the optimization, we use low-resolution images (around 40K pixels in total) and an environment map of 64x32 texels. While performance and quality depend on the sampling rates, these values proved sufficient in practice for all shown examples. For the shape-material goal, a mask is generated to contain all pixels covering the object. Image gradients are calculated considering the pixels at the right and bottom for the horizontal and vertical components respectively. At each optimization iteration, our algorithm produces a new environment map via the LBFGS-B algorithm [BLNZ03] using the implementation from [Qiu20] with its default parameters. We set the algorithm's lower bounds to a very small positive value to rule out negative values for the environment map pixels, which would result in physically incorrect lighting.

Hierarchical optimization We implemented a hierarchical solver for performance. The environment map optimization proceeds from a lower resolution version (4x2) to the original resolution (64x32). For a fast computation, we can populate the lower-resolution light-transport matrices directly by sampling the original matrix T. After the optimization of one level is finished, we linearly upsample the solution to the next level and continue.

5. Results

To show that our goal gradients are reasonable, we show that they can give a good indication of a lighting's performance with respect to shape depiction for diffuse objects. Fig. 6 shows diffuse spheres illuminated with different directional lights. The scatter plots illustrate the relation between our normal-based goal gradients and image gradients. Illuminating the sphere with a slant of 0° exhibits

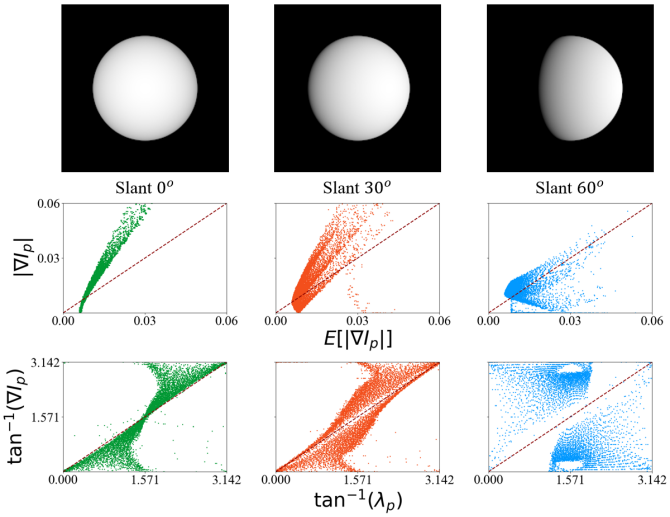

Figure 6: *Diffuse spheres under light from different angles with respect to the viewing direction. The plots compare image gradient magnitudes (top plot) and angles (bottom plot) against normal-based goal gradients magnitude $E[|\nabla I_p|]$ and orientation λ_p. The x=y line corresponds to a perfect shading gradient according to our cost function for diffuse surfaces.*

a very flat look at the center and a high gradient near the edges. While the gradient orientation generally matches the goal gradient orientations, the gradient magnitude plot shows that many pixels have a lower gradient than their goal gradient (the central pixels) - they are not depicting the shape well.

The slant 60° case has very strong highlights and shadows, that leave parts in the dark or cast shadow borders, which limits the shape perception. We see that this setting leads to gradients that do not follow the principal curvature. Further, we observe diverging gradient magnitude and orientation from our goal gradients (See Slant 60° case) indicating its low performance for shape and diffuse material depiction. We should stress that our goal gradients ignore aesthetic concerns though.

The slant 30° case gets closest to our goal gradient definition and indeed provides a more suitable shape depiction.

Our sample-based goal gradient computation takes interreflections and self-shadows into account. In Fig. 7, we show the difference between normal- and sample-based goal gradients for the given scene. Despite the high similarity between both trends, the sample-based goal gradient magnitudes are smaller than the normal-based gradients due to the considered effects. For example, interreflections near where the hair touches the face reduce the expected gradient. The Serapis model illuminated with 30° slanted directional light produces larger gradients than our sample-based goal gradients, which would indicate that the given illumination emphasizes surface orientation changes. Hair and beard exhibit hard shadows which are not ideal for shape perception. Our sample-based approach captures this characteristics. These cases are usually mitigated using fill lights in professional product photography.

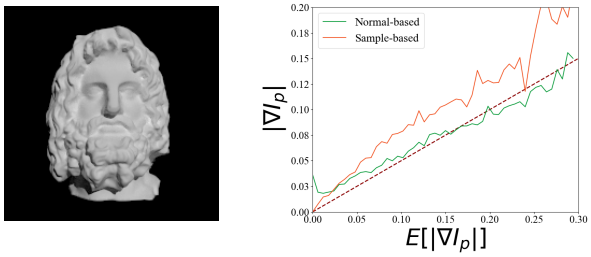

Figure 7: *Serapis bust with white diffuse material, illuminated by a directional light slant 30° with intensity 0.5. The plot shows the averaged gradient magnitudes. The dashed lines show the perfect shading gradient magnitudes according to our shape-material goal gradients (here, expected values are halved for the plot to reflect the lower light intensity).*

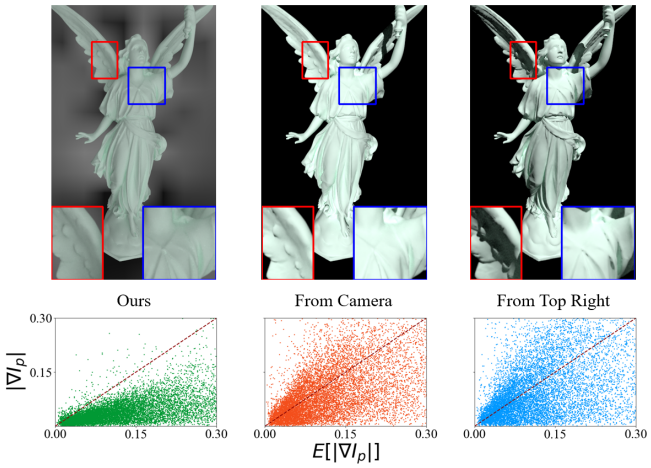

Figure 8: *Lucy statue illuminated with our solution, a light aligned with the view direction and a light coming from the top right of the camera. Cost values calculated with only our local shape and material term C_{SM_1} are 0.132, 0.156, 0.166 respectively.*

Lighting design We illustrate the potential of shape enhancement for diffuse objects and we compare our results with standard illumination directions used in studio photography [HBF12b]; a top-right light direction and a light aligned with the viewing angle. In this example and all following results, the optimization was initialized with a gray (0.5) environment map, all global weights set to 1 and the total luminosity parameter L is set to 3.

Fig. 8 shows that the frontal lighting produces a very flat shape appearance. The top-right lighting looks fine but suffers from shadows and over-saturation (i.e. the insets). Our solution creates a comparable appearance but emphasizes contours and curved regions (e.g., wings, cloth wrinkles) without exhibiting strong shadows or saturated parts.

We emphasize that our optimizer reacts to changes in the geometry well (See Fig. 9). The illumination for the edited fertility model (podium is removed from the mesh) is brighter at the bottom compared to the illumination for the original fertility model.

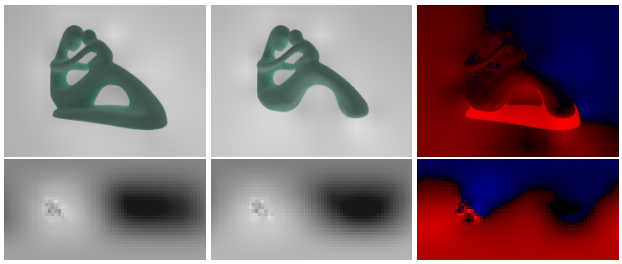

Figure 9: *Original and edited fertility (no podium) models with diffuse material are illuminated with our optimized lighting for enhanced shape depiction. Last column shows the normalized pixel differences of the two results, red and blue shows the brighter and darker parts of the 2. and 1. column respectively.*

The removal of the podium allowed the optimizer to emphasize the curviness on the legs by adding light from below.

Altering the appearance of materials is more challenging for diffuse objects than specular objects, as their BRDF basically acts as a convolution on the incoming light [DHS*05]. Mirror-like materials, in contrast, maintain high frequencies that are in the environment-map and allows changing the apparent material by changing the illumination patterns. Figure 1 shows that a larger *AG* forces the optimizer to find an environment map that enhances the depicted glossiness.

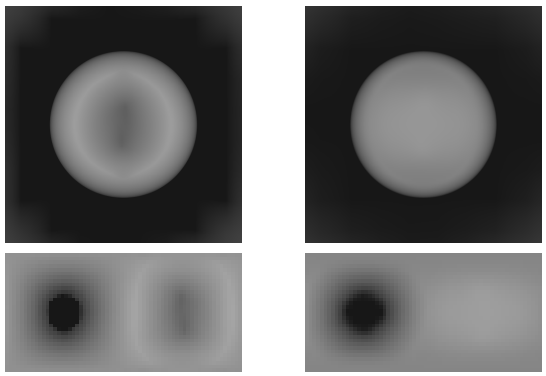

(a) $\beta_{SM_2} = 0$ **(b)** $\beta_{SM_2} = 4$

Figure 10: *Lighting is optimized to produce matte appearance for mirror spheres by setting diffuse regularizer weight, β_{SM_2}, to 0 (left) and 4 (right).*

In Fig. 10, we present our results for mirror spheres with the matte appearance design and show the effect of the diffuse regularizer term C_{SM_2} on the results. Even though both environment maps result in smooth shading, which satisfies the goal gradient term C_{SM_1} overall appearance of the result without C_{SM_2} do not look diffuse. With the help of the C_{SM_2}, we can obtain the matte appearance with only small artifacts close to the edges.

Fig. 11 compares our results to Bousseau et al. [BCRA11]. Our approach makes the depicted glossiness easily controllable, while their regularization term controls the presence of specular highlights that emphasize the glossiness. This focus on specular highlights ignores the depiction of shape. Additionally, their method sometimes produces very dark results since it ignores the overall brightness during optimization. Although manually changing the exposure brings the image to a desired level of brightness, it influences the properties of the visual features, thus gloss depiction. Nevertheless, their optimization approach is a lot faster and can be a useful start for further lighting design.

Using the painting interface, the material appearance can be well controlled, as shown in Fig. 1. Furthermore, local control is possible (Fig. 12). The result is very effective - the monkey head seems to consist of three materials, despite this not being the case. Nevertheless, pixels with differently-designed material appearance may be illuminated in the same way, making it impossible to satisfy multiple criteria at once. For example, for the monkey head model, there are specular highlights in regions with *AG*=1 around the right eye, which are caused by the criteria of the left part of the face (*AG*=4). Such situations illustrate the limitations of targeting a physically-correct lighting simulation, which exhibits the actual challenge in the real world.

We also illustrate the brightness goals that can be added using the painting interface. These annotations do not overrule shape-material goals and can lead to sophisticated designs. For the fertility model (Fig. 13), the left and the right parts of the image are designed to appear bright and dark respectively while the unpainted part of the model is designed to have a glossier appearance than matte(*AG*=3). Some bright texels in the environment map leak into the dark part due to value interpolation in the low-resolution map. There is a brightness difference between the design and the result at the top left and left of the model's background. If desired, one can adjust δ_i, the brightness goal weight for pixel i, to enforce a brighter appearance for the top left part.

Simple glass models are typically illuminated with one of the two standard lighting setups; dark and light field illumination [HBF12a]). However, more complex shapes and/or sophisticated design goals pose challenging constraints and requires custom solutions that can be achieved by our approach (Fig. 14). Brightness goals define the background color and help in creating regions, where the background should shine through the glass body. All annotations can be loose. However, since neither brightness nor shape-material design overrules the other, obtaining a complete black appearance at the center requires the brightness goal annotation and the *AG* parameter to be set to 0 for these respective regions. For $AG > 0$, highlights could appear on the black surface. Using our solution, effective glass depiction can be easily achieved.

The optimizer usually finds an optimal solution between 2 and 3 minutes (Fig. 15). With the hierarchical approach, we gain a significant convergence speed. For example, hierarchical optimization almost converges to the result approximately before the first 10 seconds for the sphere, while the standard approach takes about 50 seconds. A similar trend can be seen for both the Serapis and wine glass.

Evaluation: In order to validate the usability of our tool, we conducted an evaluation with 7 users. They had varying levels of expertise in product lighting design ranging from familiarity with a 3D design tool to being a lecturer on lighting design. After a short tutorial of the tool, they were asked to complete two tasks; free ex-

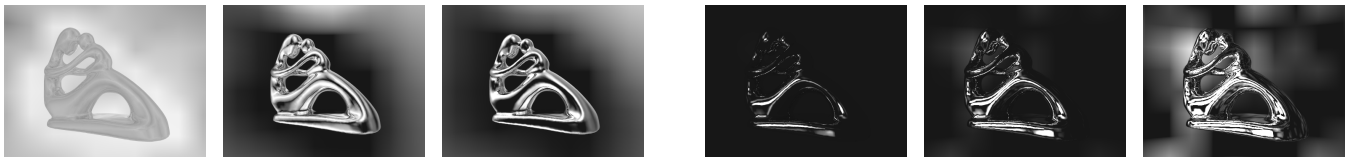

(a) *AG=1* **(b)** *AG=10* **(c)** *AG=20* **(d)** α*: 0.5* **(e)** α*: 0.005* **(f)** α*: 0.00005*

Ours Bousseau et. al.

Figure 11: *Fertility model illuminated with environment illumination that produced by our approach and Bousseau et. al. It shows how the user specified parameters required by the two approaches control the illumination.*

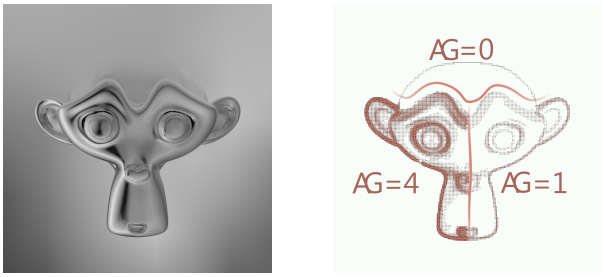

Figure 12: *Example of a varying AG using hand-painted mask. AG=0, AG=1, AG=4 guide the optimizer towards a flat, matte and highly glossy look.*

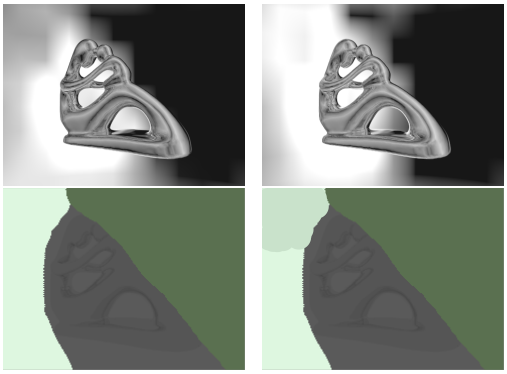

Figure 13: *A user specifies the exact brightness value by casually painting over the scene(light green and dark green indicate white and black goals respectively). AG=3 are used for the fertility model. On the right, our optimizer outputs a result whose top left is brighter achieved by changing the white goal weight* δ

ploration with the mirror monkey head and mimicking a predefined appearance for the mirror fertility model.

Although there was no time constraint, they obtained satisfying results in 6.33 and 9.43 minutes on average for the Task 1 and 2 respectively. Then, we asked whether they find the tool easy to learn and whether the tool meet their design goals where they can rate on a scale of 1 to 5. Three of four inexperienced users who rated 2 or 3 for the experience level out of 5, found our solution easy to learn (5, 5, 4) and easy to use (4, 4, 5). The other inexperienced user rated easy to learn (5) but found it difficult to control the optimizer (1) via the provided design tools. Their main difficulty stems from missing

Figure 14: *Even though the results without brightness goals produces contours with sharp contrast, the use of brightness annotations guided our optimizer to solutions that realize the widespread product photography principles (the wine glass uses AG=7, while the bottle uses AG=5).*

feedback from the system when conflicts arise in the design, which can lead to contradictions that the solver cannot resolve.

In the end, we asked open questions on the experience and the points to be improved. Experienced participants expressed that they find our solution extremely useful even though they would not completely rely on it since it limits their freedom and it requires a completely different approach to their typical work. However they suggested various ways in which it can already improve their standard workflow. First of all it can give various ideas before starting the actual lighting design. Secondly, it can produce quick drafts that can accelerate discussions with customers. Lastly, it can also be useful for educational purposes.

5.1. Limitations

Our solution only indirectly targets specular highlights. Fig. 16 shows that this solution, similar to Bousseau et al., has its limitations for simple geometries like a sphere. Our optimizer produces high contrast and sharp highlights through large gradients but the results do not appear glossy for simple geometries. It supports that sharp and high contrast are not sufficient cues for glossy appearance. Previous studies [FDA03; vAWP16] revealed, that humans perceive simple geometries to be glossy when the reflections represent statistics of natural environments.

Another limitation is shown in Fig. 2 (right). The optimizer reacted well on different appearance designs and found environment maps that highlight the respective parts as desired, leading to a high contrast at the contours with a uniform background and a small specular highlight at the top right of the body (See Fig. 17)). Nevertheless, the specular highlights could be better defined and some

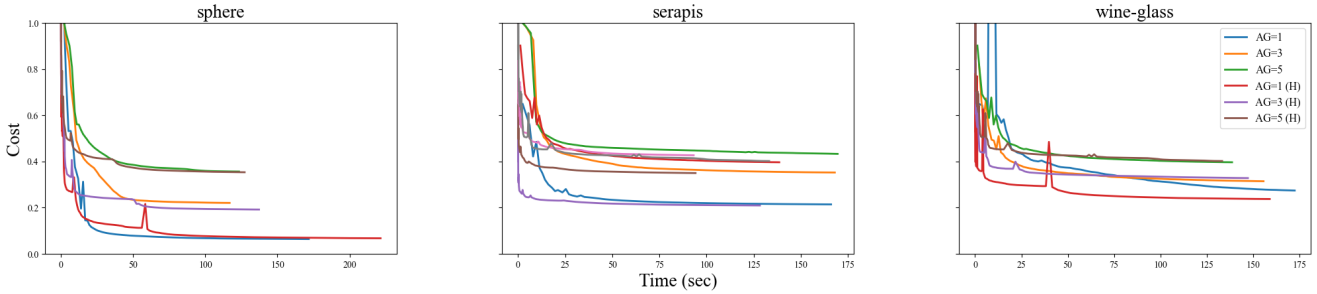

Figure 15: *Shows the evolution of the cost in time (seconds). Each object is optimized with different AG values; with and without hierarchical optimization approach.*

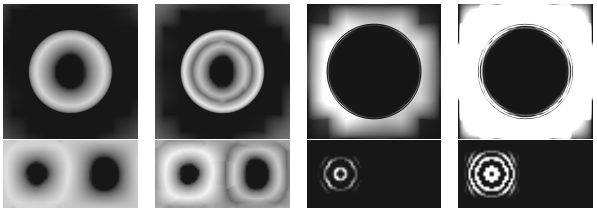

(a) *AG=10* **(b)** *AG=20* **(c)** α*: 0.5* **(d)** α*: 0.00005*

Ours Bousseau et. al.

Figure 16: *Despite its simplicity, a sphere is a difficult case. For higher AG values (glossy appearance design), our solution produces large gradients but no glossy appearance. Previous work [BCRA11] produces similar results for such special cases.*

(a) *Highlight top left* **(b)** *Highlight top right* **(c)** *Difference*

Figure 17: *We defined higher AG values for the contours, the top-left, and top-right part of the body as an attempt to realize the bottle appearance in Fig. 2 right. The latter has a specular highlight at the top right of the bottle body. The left two images show the obtained results for the shown shape-material designs. The last column shows the normalized difference of the two results, red and blue shows the brighter and darker parts of the 2. and 1. column respectively.*

spurious specular highlights exist. One potential reason is that the low-resolution environment maps reaching their limit and leading to a local minimum. This is a limitation of the method because higher resolutions require additional memory and compute time.

Finally, texture, as well as small-scale material changes, can produce strong gradients that are not in accordance with the shape. Our method targets nontextured objects, as it might result in undesired material appearances when the texture induces strong changes. Especially if textures encode specular material properties, the appearance can change drastically, which is difficult to handle by our solution.

6. Conclusion

Lighting design emphasizing shape and material is very common but the task is inherently difficult, as both elements influence each other. The key insight is to link shape orientation and curvature with shading via a cost function derived for Lambertian materials. We show that specularity cues can be enhanced using these constraints as well. Our solution simplifies this complex aspect of lighting design and supports the creation of well-suited, yet complex environment maps with little effort for the user. The fact that our system optimizes environmental lighting based on all user-specified constraints simultaneously is well adapted to capture the complex interrelations between different annotations. Compared to previous work, we were able to maintain a high level of control by allowing global goals and local influence on the parameters. We demonstrated various challenging scenarios with complex models and difficult design targets that our system could solve successfully. Our user study shows that image based lighting design is very easy to learn and practical for novice users. With its unique qualities, it is an interesting addition to the lighting-design toolbox for both new starters and experienced users.

In the future, we want to explore various cost functions that focus directly on special material types, such as fabrics, which show varying visual features depending on the viewing conditions, and transparent materials. Another direction that deserves further research is extending our method to support colored environment map designs. We also would like to investigate the potential of our shape-material metric in a dynamic illumination setup.

7. Acknowledgments

This work was supported by DyViTo that is funded by the European Union's Horizon 2020 programme under grant agreement No 765121. The authors would like to thank the reviewers for the valuable comments and suggestions.

References

[ADW04] ANRYS, FREDERIK, DUTRÉ, PHILIP, and WILLEMS, YVES D. "Image-based lighting design". *Proceedings of the 4th IASTED International Conference on Visualization, Imaging, and Image Processing*. 2004, 15 2, 3, 5.

[AK09] ANDERSON, BARTON L. and KIM, JUNO. "Image statistics do not explain the perception of gloss and lightness". *Journal of Vision* 9.11 (Oct. 2009), 10–10. ISSN: 1534-7362. DOI: 10.1167/9.11.10 2.

[BCRA11] BOUSSEAU, ADRIEN, CHAPOULIE, EMMANUELLE, RAMAMOORTHI, RAVI, and AGRAWALA, MANEESH. "Optimizing Environment Maps for Material Depiction". *Comput. Graph. Forum* 30 (June 2011), 1171–1180. DOI: 10.1111/j.1467-8659.2011.01975.x 2, 3, 7, 9.

[BLNZ03] BYRD, RICHARDH, LU, PEIHUANG, NOCEDAL, JORGE, and ZHU, CIYOU. "A Limited Memory Algorithm for Bound Constrained Optimization". *SIAM Journal on Scientific Computing* 16 (Feb. 2003). DOI: 10.1137/0916069 5.

[BPB13] BOYADZHIEV, IVAYLO, PARIS, SYLVAIN, and BALA, KAVITA. "User-assisted Image Compositing for Photographic Lighting". *ACM Transactions on Graphics (TOG)* 32 (July 2013). DOI: 10.1145/2461912.2461973 3.

[Bra00] BRADSKI, G. "The OpenCV Library". *Dr. Dobb's Journal of Software Tools* (2000) 5.

[BZ96] BRETON, P. and ZUCKER, S.W. "Shadows and shading flow fields". *Proceedings CVPR IEEE Computer Society Conference on Computer Vision and Pattern Recognition*. 1996, 782–789. DOI: 10.1109/CVPR.1996.517161 2, 3.

[CF07] CANIARD, FRANCK and FLEMING, ROLAND W. "Distortion in 3D Shape Estimation with Changes in Illumination". *Proceedings of the 4th Symposium on Applied Perception in Graphics and Visualization*. APGV '07. Tubingen, Germany: Association for Computing Machinery, 2007, 99–105. ISBN: 9781595936707. DOI: 10.1145/1272582.1272602 2.

[DBM07] DOERSCHNER, K., BOYACI, H., and MALONEY, L.T. "Testing limits on matte surface color perception in three-dimensional scenes with complex light fields". *Vision Research* 47.28 (2007), 3409–3423. ISSN: 0042-6989. DOI: 10.1016/j.visres.2007.09.020 2.

[DHS*05] DURAND, FRÉDO, HOLZSCHUCH, NICOLAS, SOLER, CYRIL, et al. "A Frequency Analysis of Light Transport". *ACM Transactions on Graphics* 24 (July 2005). DOI: 10.1145/1073204.1073320 7.

[FA07] FATTAL, RAANAN and AGRAWALA, MANEESH. "Multiscale Shape and Detail Enhancement from Multi-light Image Collections". *ACM Trans. Graph.* 26 (July 2007). DOI: 10.1145/1276377.1276441 3.

[FDA03] FLEMING, ROLAND, DROR, RON, and ADELSON, EDWARD. "Real-world illumination and the perception of surface reflectance properties". *Journal of vision* 3 (Feb. 2003), 347–68. DOI: 10.1167/3.5.3 2, 8.

[FTA04] FLEMING, ROLAND, TORRALBA, ANTONIO, and ADELSON, EDWARD. "Specular reflections and the perception of shape". *Journal of vision* 4 (Oct. 2004), 798–820. DOI: 10.1167/4.9.10 2.

[GLCC18] GALVANE, QUENTIN, LINO, C., CHRISTIE, MARC, and COZOT, R'MI. "Directing the Photography: Combining Cinematic Rules, Indirect Light Controls and Lighting-by-Example". *Computer Graphics Forum* 37 (Oct. 2018), 45–53. DOI: 10.1111/cgf.13546 3.

[HBF12a] HUNTER, FIL, BIVER, STEVEN, and FUQUA, PAUL. "7 - The Case of the Disappearing Glass". *Light Science and Magic (Fourth Edition)*. Ed. by HUNTER, FIL, BIVER, STEVEN, and FUQUA, PAUL. Fourth Edition. Boston: Focal Press, 2012, 156–190. ISBN: 978-0-240-81225-0. DOI: 10.1016/B978-0-240-81225-0.00007-9 2, 7.

[HBF12b] "Front Matter". *Light Science and Magic (Fourth Edition)*. Ed. by HUNTER, FIL, BIVER, STEVEN, and FUQUA, PAUL. Fourth Edition. Boston: Focal Press, 2012, i–ii. ISBN: 978-0-240-81225-0. DOI: 10.1016/B978-0-240-81225-0.00017-1 1, 2, 6.

[JDA07] JUDD, TILKE, DURAND, FRÉDO, and ADELSON, EDWARD. "Apparent Ridges for Line Drawing". *ACM Trans. Graph.* 26 (July 2007), 19. DOI: 10.1145/1276377.1276401 3.

[JP94] JOHNSTON, ALAN and PASSMORE, PETER. "Shape from shading. I: Surface curvature and orientation". *Perception* 23 (Feb. 1994), 169–89. DOI: 10.1068/p230169 2.

[KDKT01] KOENDERINK, JAN, DOORN, ANDREA, KAPPERS, ASTRID, and TODD, JAMES. "Ambiguity and the 'Mental Eye" in pictorial relief". *Perception* 30 (Feb. 2001), 431–48. DOI: 10.1068/p3030 2.

[KHA*18] KUNSBERG, BENJAMIN, HOLTMANN-RICE, DANIEL, ALEXANDER, EMMA, et al. "Colour, contours, shading and shape: Flow interactions reveal anchor neighbourhoods". *Interface Focus* 8 (Aug. 2018), 20180019. DOI: 10.1098/rsfs.2018.0019 2.

[KMA11] KIM, J., MARLOW, PHILLIP J., and ANDERSON, B. "The perception of gloss depends on highlight congruence with surface shading." *Journal of vision* 11 9 (2011) 2.

[KP09] KERR, WILLIAM B. and PELLACINI, FABIO. "Toward Evaluating Lighting Design Interface Paradigms for Novice Users". *ACM Trans. Graph.* 28.3 (July 2009). ISSN: 0730-0301. DOI: 10.1145/1531326.1531332 2, 5.

[LGCB14] LÉON, VINCENT, GRUSON, ADRIEN, COZOT, RÉMI, and BOUATOUCH, KADI. "Automatic Aesthetics-based Lighting Design with Global Illumination". (Jan. 2014) 3.

[LHV06] LEE, CHANG, HAO, XUEJUN, and VARSHNEY, AMITABH. "Geometry-dependent lighting". *IEEE transactions on visualization and computer graphics* 12 (Apr. 2006), 197–207. DOI: 10.1109/TVCG.2006.30 3.

[MA14] MOONEY, SCOTT W.J. and ANDERSON, BARTON L. "Specular Image Structure Modulates the Perception of Three-Dimensional Shape". *Current Biology* 24.22 (2014), 2737–2742. ISSN: 0960-9822. DOI: 10.1016/j.cub.2014.09.074 2.

[MNSA07] MOTOYOSHI, ISAMU, NISHIDA, SHIN'YA, SHARAN, LAVANYA, and ADELSON, EDWARD. "Image statistics and the perception of surface qualities". *Nature* 447 (June 2007), 206–9. DOI: 10.1038/nature05724 2.

[PBMF07] PELLACINI, FABIO, BATTAGLIA, FRANK, MORLEY, R., and FINKELSTEIN, ADAM. "Lighting with paint". *ACM Trans. Graph.* 26 (June 2007). DOI: 10.1145/1243980.1243983 3.

[Pel10] PELLACINI, FABIO. "envyLight: An Interface for Editing Natural Illumination". *ACM Transactions on Graphics (TOG)* 29 (July 2010), 34. DOI: 10.1145/1778765.1778771 3.

[PFG00] PELLACINI, FABIO, FERWERDA, JAMES, and GREENBERG, DONALD. "Toward a Psychophysically-based Light Reflection Model for Image Synthesis". Vol. 2000. Jan. 2000, 55–64. DOI: 10.1145/344779.344812 2.

[PH10] PHARR, MATT and HUMPHREYS, GREG. *Physically Based Rendering, Second Edition: From Theory To Implementation*. 2nd. San Francisco, CA, USA: Morgan Kaufmann Publishers Inc., 2010. ISBN: 0123750792 5.

[PRJ97] POULIN, P., RATIB, K., and JACQUES, M. "Sketching shadows and highlights to position lights". *Proceedings Computer Graphics International*. 1997, 56–63. DOI: 10.1109/CGI.1997.601272 3.

[Qiu20] QIU, YIXUAN. *LBFGSpp*. https://github.com/yixuan/LBFGSpp. 2016-2020 5.

[SL01] SHACKED, RAM and LISCHINSKI, DANI. "Automatic Lighting Design Using a Perceptual Quality Metric". *Comput. Graph. Forum* 20 (Sept. 2001). DOI: 10.1111/1467-8659.00514 3.

[SN18] SAWAYAMA, MASATAKA and NISHIDA, SHIN'YA. "Material and shape perception based on two types of intensity gradient information". *PLOS Computational Biology* 14.4 (Apr. 2018), 1–40. DOI: 10.1371/journal.pcbi.1006061 2.

[TN19] TODD, JAMES and NORMAN, J. "Reflections on glass". *Journal of Vision* 19 (Apr. 2019), 26. DOI: 10.1167/19.4.26 2.

[vAWP16] Van ASSEN, JAN JAAP R., WIJNTJES, MAARTEN W. A., and PONT, SYLVIA C. "Highlight shapes and perception of gloss for real and photographed objects". *Journal of Vision* 16.6 (Apr. 2016), 6–6. ISSN: 1534-7362. DOI: 10.1167/16.6.6 2, 8.

[WAKB09] WILLS, JOSH, AGARWAL, SAMEER, KRIEGMAN, DAVID, and BELONGIE, SERGE. "Toward a Perceptual Space for Gloss". *ACM Trans. Graph.* 28 (Aug. 2009). DOI: 10.1145/1559755.1559760 2.

[WK13] WANG, LEI and KAUFMAN, ARIE E. "Lighting System for Visual Perception Enhancement in Volume Rendering". *IEEE Transactions on Visualization and Computer Graphics* 19.1 (2013), 67–80. DOI: 10.1109/TVCG.2012.91 3.

[WP10] WIJNTJES, MAARTEN and PONT, SYLVIA. "Illusory gloss on Lambertian surfaces". *Journal of vision* 10 (July 2010), 13. DOI: 10.1167/10.9.13 2.

[WVBT16] WAMBECKE, JÉRÉMY, VERGNE, ROMAIN, BONNEAU, GEORGES-PIERRE, and THOLLOT, JOËLLE. "Automatic Lighting Design from Photographic Rules". *Eurographics Workshop on Intelligent Cinematography and Editing*. Ed. by CHRISTIE, M., GALVANE, Q., JHALA, A., and RONFARD, R. The Eurographics Association, 2016. ISBN: 978-3-03868-005-5. DOI: 10.2312/wiced.20161094 3.

[ZdRBP19] ZHANG, FAN, de RIDDER, HUIB, BARLA, PASCAL, and PONT, SYLVIA. "A systematic approach to testing and predicting light-material interactions". *Journal of Vision* 19.4 (Apr. 2019), 11–11. ISSN: 1534-7362. DOI: 10.1167/19.4.11 2.